CANADA
DEPARTMENT OF MINES AND RESOURCES
MINES, FORESTS, AND SCIENTIFIC SERVICES BRANCH

PUBLICATIONS

OF THE

Dominion Observatory

OTTAWA

Vol. XI, No. 8

A Phenomenological Theory of Radar Echoes from Meteors

By

D. W. R. McKinley and Peter M. Millman

Reprinted from the PROCEEDINGS OF THE I.R.E., Vol. 37, pp. 364-375, 1949

A Phenomenological Theory of Radar Echoes from Meteors*

D. W. R. McKINLEY†, FELLOW, IRE, AND PETER M. MILLMAN‡

Summary—**The Dominion Observatory and the National Research Council, Ottawa, Canada, have undertaken a program of combined visual, photographic, and radar observations of meteors. The observational data is summarized, and general conclusions have been drawn.**

The radar echoes obtained from meteors have been classified into basic types according to their appearance on the range-time record of the radar display. These types include echoes indicating approach, or recession, or both. Other observed features are: durations of echoes up to several minutes, complexity of structure for echoes from brighter meteors, and appreciable delays in the appearance of the echoes.

A phenomenological theory is proposed, involving a number of postulates concerning the physical conditions in an *M* region in the upper atmosphere. A kinetic-energy mechanism, together with an ultraviolet radiation mechanism, are suggested to account for the ionization produced by the meteor. In the *M* region are visualized striae, or patches, which form a fine structure such that, within the striae, the physical properties of the atmosphere emphasize the creation and maintenance of meteoric ionization as compared to the ionization produced in the intervening spaces. A qualitative explanation for all the observed echo forms is advanced on the above hypothesis. The results of other investigators on different wavelengths are consistent with this analysis.

Introduction

EVER SINCE the first tentative suggestions were made by Pickard,[1] Skellett,[2,3] and others that short-duration *E*-region radar reflections might be due to meteoric ionization, considerable interest has been aroused in many quarters and a great deal of observational and theoretical work has been done. The result is that, at this date, there is no serious doubt that meteors actually produce transient echoes which are obtained from heights near the *E* region. The evidence is overwhelming: the diurnal and annual echo rates vary with the visual meteor rates; the rates increase during the well-known visual showers; many definite coincidences have been obtained between the stronger echoes and the brighter visual meteors.

Up to the present, however, the literature does not show that the correlation between the visual meteors and the radar echoes has been carried out in as thorough a manner as might be desired. With the object of giving particular attention to this phase of the problem, a combined project was initiated in August, 1947, at Ottawa under the auspices of the Dominion Observatory and the National Research Council. The combined observations have so far been made on the Perseid shower of August, 1947,[4] on the Geminid shower of December, 1947,[5] and on the Lyrid shower of April, 1948.[5] The radar equipment has been operated alone at other times. The meteor-shower periods are selected for the combined work chiefly for the reason that direction of motion of the shower meteors is known. Hence, from visual or photographic observations made at a single point on the earth's surface, not only can the position of a meteor trail[6] in the sky be found but, if that meteor is identified as a shower meteor, the angle between the meteor's path and the line of sight can be determined. Further, the geocentric velocity is also known for most of the annual showers, and the number of meteors in the sky during a shower is considerably greater than on a nonshower night.

In the program on which this paper is based, the visual observations were carried out by a team of six or more observers, and the reduction of their data yielded meteor positions with an average error in the neighborhood of 3°. Direct and spectrographic cameras were also operated, and when photographs of the brighter meteors were available, the error in the observed position was of the order of 0°.05. The timing error of the visual meteors was about ½ to 1 second. The times were recorded both by a recording observer associated with the observing group, and by an Esterline-Angus multipen recorder with individual pens remotely controlled by each observer. During the Lyrid shower, push buttons were connected to an illuminated indicator which marked the radar film directly.

The parameters of the radar system during the Perseid shower were as follows: frequency, 32.7 Mc; peak power, 150 kw; pulse length, 8 microseconds; receiver sensitivity, 5×10^{-14} watt; single half-wave horizontal dipoles on both transmitter and receiver, each mounted a quarter-wave above the ground plane, both dipoles

* Decimal classification: R113.415×R537. Original manuscript received by the Institute, June 21, 1948; revised manuscript received, September 23, 1948.

† Radio and Electrical Engineering Division, National Research Council, Ottawa, Canada.

‡ Dominion Observatory, Department of Mines and Resources, Ottawa Canada.

[1] G. W. Pickard, "A note on the relation of meteor showers and radio reception," PROC. I.R.E., vol. 19, pp. 1166–1170; July, 1931.

[2] A. M. Skellett, "The effect of meteors on radio transmission through the Kennelly-Heaviside layer," *Phys. Rev.*, vol. 37, p. 1668; June 15, 1931.

[3] A. M. Skellett, "The ionizing effect of meteors in relation to radio propagation," PROC. I.R.E., vol. 20, pp. 1933–1940; December, 1932.

[4] Peter M. Millman, D. W. R. McKinley, and M. S. Burland, "Combined radar, photographic and visual observations of the 1947 Perseid meteor shower," *Nature*, vol. 161, pp. 278–280; February 21, 1948.

[5] Peter M. Millman and D. W. R. McKinley, "A note on four complex meteor radar echoes," *Jour. Roy. A. Soc. Can.*, vol. 42, pp. 121–130; May and June, 1948.

[6] In this paper, we define *meteor path* as the line of motion of a meteor described in a three-dimensional co-ordinate system referred to the earth. *Meteor trail* is the meteor path projected on the celestial sphere, as seen by the observer.

oriented north-south. The power was increased to about 400 kw peak, with a 12-microsecond pulse length, just prior to the Geminid shower, with the other parameters remaining approximately the same. An A-scope display was used for monitoring, and a range-time display on a long-delay-screen cathode-ray tube was employed for recording and timing the radar echoes. In August, the range-time display was continuously photographed with a single-shot movie camera open for 1-minute intervals. Since November, a continuously moving film camera has been employed with a stationary, intensity-modulated range trace. Timing seconds pulses were available from the Dominion Observatory's time service, radio station CHU. Starting in December, these seconds pulses have been applied directly to the range trace. The same pulses were made audible for use by the visual observers. The timing error of the radar echoes was of the order of one-quarter of a second or better, and the combined error of visual and radar timing was thus of the order of one second, on the average.

The experimental data obtained from these showers have been described briefly elsewhere, and more complete accounts are being prepared for publication. However, it was felt that several interesting conclusions could be drawn from this work without recounting the vast amount of small detail involved in making and reducing the observations. This paper summarizes the results and outlines a phenomenological theory of the mechanics of radar reflections from meteors.

Several theories of meteoric ionization and the radar reflections obtained from the meteor trails have been advanced.[7-9] One of the salient points in these discussions is the fact, clearly demonstrated experimentally, that the trail of ionization behaves as a long, thin reflecting cylinder immediately after the passage of the meteor. Thus the most efficient reflection will be obtained from a meteor when its path is normal to the line of sight. Our observations have added further confirmation to the large amount of data verifying this normal reflection law. However, we should like to point out that this law applies only *immediately after* the passage of the meteor, as we believe that the character of the radar echoes and the mechanics of reflection change radically with time and with the orientation of the meteor path with respect to the line of sight. That is, while the bulk of the small meteor echoes observed are probably seen as a consequence of the normal reflection law, the larger meteors definitely produce complicated echoes which are not explained by this law.

Statistical Data from the Radar Observations—Determination of Shower Radiant

We shall define the angle α as the angle between the line drawn from the meteor to the observer (measured from the midpoint of the visual path unless otherwise specified) and the meteor path. For example, $\alpha = 90°$ defines a meteor traveling normal to the line of sight. Values of α less than 90° will represent meteors approaching the observer, while values greater than 90° denote meteors receding from the observer. For every recorded visual meteor, the position of the trail can be written down in terms of the azimuthal angle A and the angle of elevation h. If the visual meteor was identified as a shower meteor (by projecting its trail back to the shower radiant),[10] then it was possible to compute the angle α. Only shower meteors were used in these correlations.

It is of interest to study the distribution of the angle α over the visible sky, for a meteor radiant at a given angle of elevation h. For this purpose we shall assume, tentatively, that the region in which the meteors occur is a thin layer at a height of 100 km above a flat earth. The assumption of a curved earth complicates the calculations unnecessarily, as the corrections introduced are not significant at this stage. (When discussing elevation-range correlations it is desirable to take into account the curvature of the earth, and this has been done.) The geometry of the situation is outlined in Fig. 1 (a) (elevation). R_{max} is the maximum slant range available on the radar display.[11] The curves, α = constant, are de-

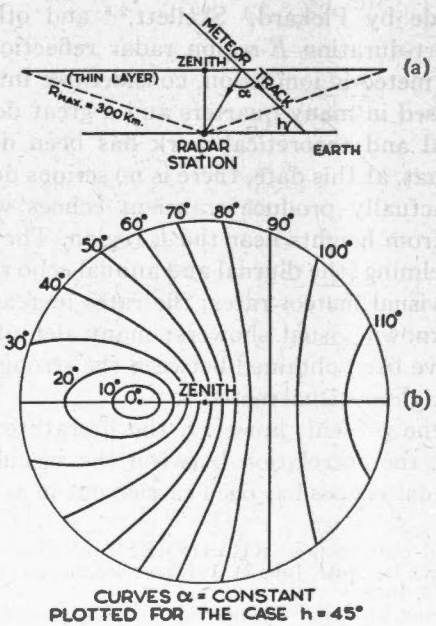

Fig. 1—(a) Elevation. (b) Plan.

[7] E. W. Allen, Jr., "Reflections of very-high-frequency radio waves from meteoric ionization," PROC. I. R. E., vol. 36, pp. 346–352; March, 1948.

[8] J. S. Hey and G. S. Stewart, "Radar observations of meteors," *Proc. Phys. Soc.*, vol. 59, pp. 858–883; September, 1947.

[9] A. C. B. Lovell and J. A. Clegg, "Characteristics of radio echoes from meteor trails: I. The intensity of the radio reflections and electron density in the trails," *Proc. Phys. Soc.*, vol. 60, pp. 491–498; May, 1948.

[10] A meteor radiant is defined as the point on the celestial sphere which is the origin of the meteor trail when the meteor path is projected back to infinity.

[11] The terms "range" or "slant range" define the distance from the observer to the target.

fined by the intersection of the layer with the cone of half-angle α, apex at the radar station, and axis directed toward the radiant. These curves, which are conic sections, are plotted in Fig. 1 (b) (plan) for 10° increments in α and for an arbitrary radiant elevation $h=45°$. The particular case $\alpha=90°$ is of especial interest. From Fig. 1 it is apparent that the perpendicular distance from the radar station to the straight line $\alpha=90°$ is given by $R_{min}=100/\cos h$.

We shall examine briefly the statistical information available in the radar records alone. In this discussion, a typical shower period, December 12 and 13, 1947 (the maximum of the Geminid shower), and a typical nonshower or standard period, February 5 and 6, 1948, will be selected as samples. The expression "standard period" is open to question, since the minor shower radiants are so numerous it is difficult to select a time interval in which meteors could be described as wholly sporadic. However, the statistical effects of the minor radiants are small and tend to average out. Hourly counts were made of the number of echoes in arbitrarily selected slant-range classes of the range-time records. The numbers in each range class were further broken down into groups containing short echoes less than 1 second in duration, and groups containing echoes 1 second and longer. The hourly average ranges of the short echoes, of the long echoes, and of all echoes were then calculated.

Let us first analyze the data for the standard period. The hourly rates (all echoes) are plotted in Fig. 2. This

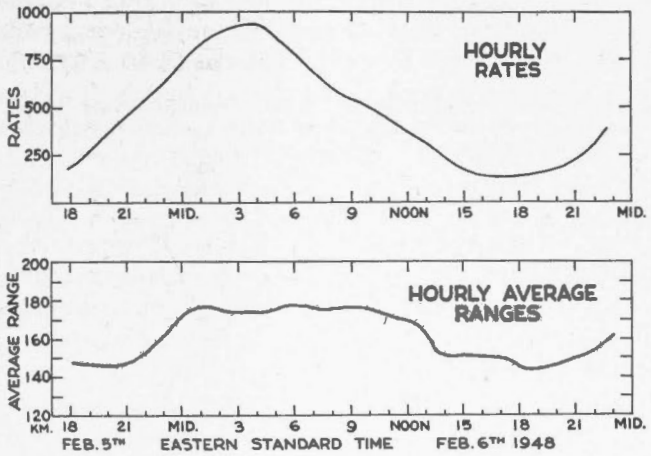

Fig. 2—Typical standard-period curves.

rate curve is in general agreement with other meteor echo counts, and with the usual diurnal variation in number of visual meteors. Next, Fig. 2 also shows the hourly average range of all echoes for the standard period. If we separate the data into two periods, period A from 0000 to 1000 hours (7,500 echoes) and period B from 1300 to 2300 hours (4,000 echoes), and plot the frequency distribution in range, we get the curves shown in Fig. 3. The change in shape of the curves could be explained by a depression of the over-all radar parameters of several db during the period B, but this possibility was checked and eliminated. The probable explanation is that the morning echoes, as well as being more numerous, are actually stronger (therefore, visible at a greater range) than the evening echoes, since the average geocentric velocity of nonshower meteors is highest at about 0600 hours. A meteoroid of a given physical size presumably produces ionization proportional to some function of its geocentric velocity.

The curves in Fig. 3 can be represented by semi-empirical equations of an exponential form if certain assumptions are made concerning the reflecting proper-

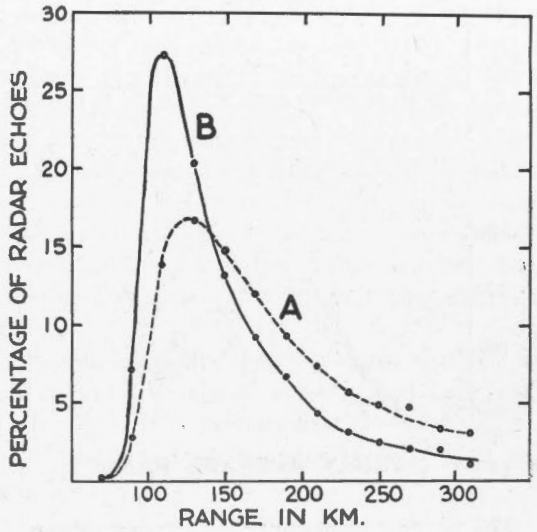

Fig. 3—Standard-period range-distribution curves.

ties of the meteoric ionization clouds and their distribution in space. However, as several widely divergent theoretical assumptions led to the same distribution curves, no significant conclusions were reached.

Let us now examine our typical shower period. The radar parameters were the same during the standard period and the shower period, so that many of the variables can be eliminated in comparing the observational data. The hourly rates of all echoes during the shower period are plotted in Fig. 4, together with the standard hourly rates from Fig. 2 for comparison purposes. A pronounced minimum in the shower period curve at 0200 hours is obvious. In Fig. 4 we have also plotted the hourly average ranges during the shower period. The solid curve is for all echoes, the dotted curve for the short echoes, and the dashed curve for the long echoes. The trend is the same for all three curves, each showing a minimum at 0210 hours. The long echoes show a consistently greater average range than the short ones, and this might be expected from noting that a long echo is usually a strong echo (the converse is not necessarily true).

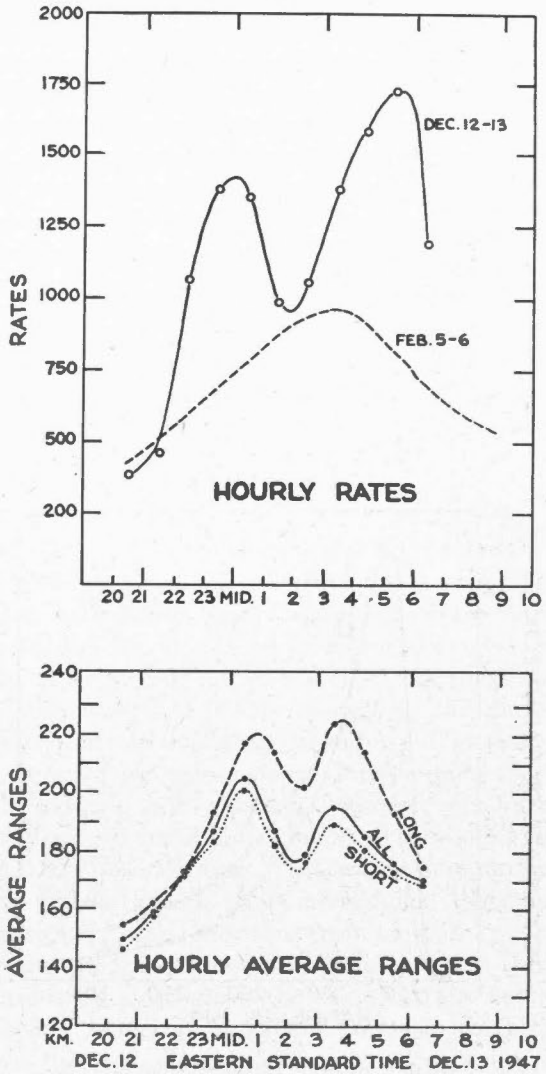

Fig. 4—Geminid shower period curves.

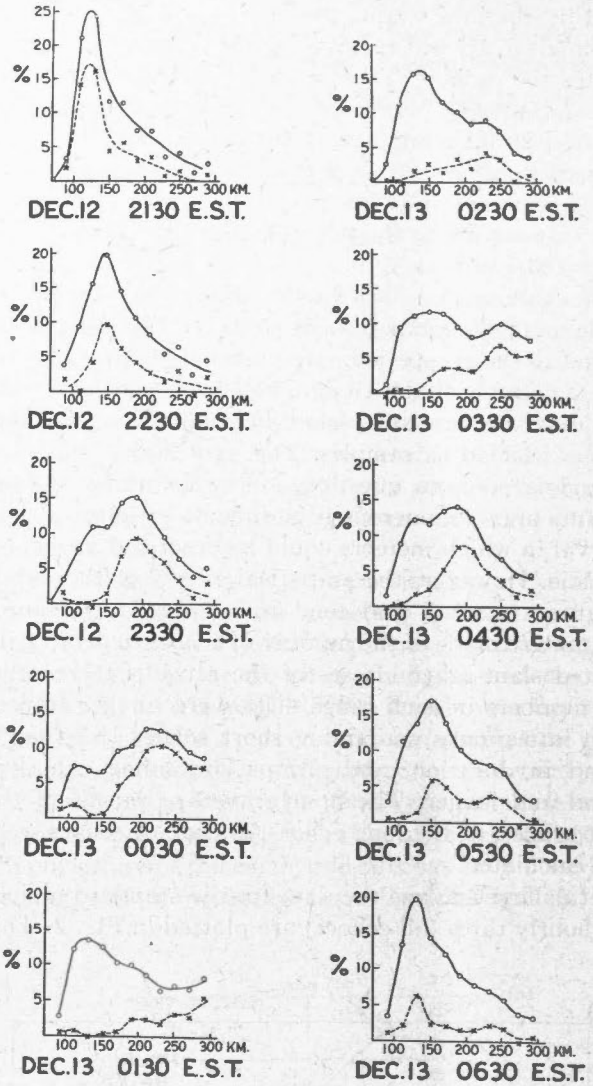

Fig. 5—Hourly range-distribution curves, Geminid shower period. Solid curves—observed distribution of all echoes; dashed curves—calculated distribution of Geminid echoes.

In Fig. 5 the solid curves show the hour-by-hour range distributions for the shower period, plotted for all echoes. We now make the assumption that the progressive deviations in shape of these shower period curves from the standard curves for the corresponding hours are due to the presence of the shower echoes, and then attempt to segregate the shower echoes from the standard background of sporadic echoes. From Fig. 4 a rough estimate of the hourly ratios of shower rates to standard rates is available and can be verified by fitting "rubber" standard-distribution curves inside each of the curves of Fig. 5. By subtracting the estimated percentages of sporadic echoes from the shower curves, the dotted curves of Fig. 5 have been obtained. These indicate the range distributions of the pure shower echoes.

It has been noted above that, in most cases, the meteoric ionization reflects the radar wave best when $\alpha = 90°$. From Fig. 1 it is seen that the curve $\alpha = 90°$ is a straight line across the thin ionizing layer, with the minimum slant range given by $R_{min} = 100/\cos h$. In practice, there will be a spread in range and height of shower meteor echoes about this line. However, the greatest concentration of meteor echoes will be found in a small region around the line. Attenuation with range will reduce the contributions from meteors at the extremities, so that most of the echoes should be seen at about the range R_{min}. In other words, the ranges of the maxima of the pure shower curves should be a good first approximation to use in the above formula. The hourly values of h for the Geminid radiant are calculated in this way and plotted as points on Fig. 6.

The values of h in the neighborhood of 0100 to 0300 hours are in doubt, and it is obvious from Fig. 5 that the maximum range of 300 km available on the display was not great enough to permit a reliable determination of the maxima for those hours. This fact also accounts for the fortuitous sharpness of the dips in the hourly-rate and average-range curves, Fig. 4. By drawing a smooth curve (solid line, Fig. 6) through the remaining points, it is possible to determine the maximum eleva-

tion of the radiant. The time of the maximum elevation also can be estimated from this curve, but it can be obtained more accurately from either the average-range

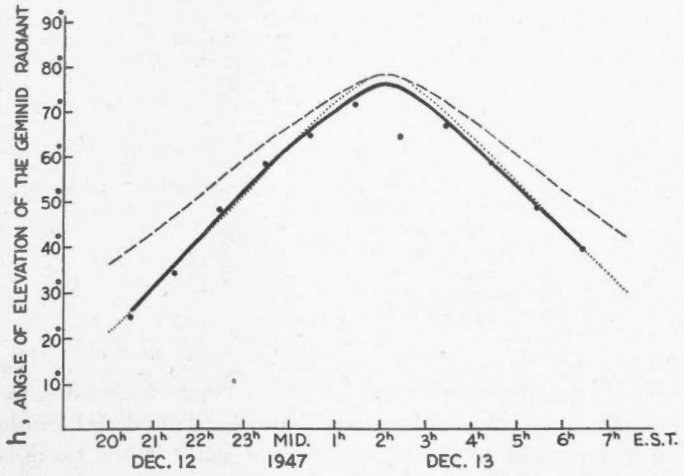

Fig. 6—Hourly angle of elevation of Geminid radiant; solid curve—radar data; dotted curve—computed for radiant at R. A. 112°, declination +33°; dashed curve—computed for radiant at R. A. 112°, declination +57°.

or the hourly-rate curves. The dotted curve in Fig. 6 shows the computed hourly elevation of the apparent Geminid radiant[12] with a maximum elevation of 78° at Ottawa, plotted by assuming the radiant at right ascension 112°, declination +33°, a position taken from the best available data.[13] The dashed curve shows the hourly elevation of an alternative radiant, right ascension 112°, declination +57°, which also has a maximum elevation of 78° at Ottawa. It is apparent that the radar observations agree with the curve for the first radiant rather than that for the second, and hence there is no ambiguity.

The radar determination of the Geminid radiant yielded a maximum elevation of 76° at 0208 hours EST, giving a position at right ascension 112°, declination +31°, in good agreement with that determined by Whipple. The probable error of the radar radiant is between 2° and 3°. One can thus determine the position of the radiant of a strong shower by statistical analysis of radar echoes, using an antenna which is effectively nondirectional and without moving the antenna or measuring angles. The method is applicable to daytime showers as well, but might be difficult to apply where several radiants are simultaneously active.

Correlation of the Visual Observations with the Radar Data

The list of visual shower meteors was compared with the radar film with a view to establishing coincidences in time. It was quickly found that such coincidences had most significance in the cases where the visual meteor was relatively bright and/or the radar trace was several seconds long. In fact, for the vast bulk of the short-duration radar echoes which coincided with visual meteors within an arbitrary time interval (e.g., plus or minus 4 seconds), it was found that the correlation was very nearly what one might expect if one assumed that the visual and radar meteors were completely independent of each other. Preliminary correlation criteria, based on time coincidence, radar-echo duration, and visual brightness of the meteor, were applied to isolate rather more than one hundred examples from 3,700 radar echoes and 1,100 visual meteors recorded during the Perseid shower. A further test was applied to the selected list. The slant range of the radar echo was used with the elevation angle of the associated visual meteor to calculate the height of the midpoint of the meteor path above a curved earth. If the height seemed reasonable, on the preliminary assumption that most meteor echoes occur between 80 and 120 km, the correlation was accepted. A list of 101 such visual-radar meteors was eventually produced from the Perseid data, and statistical considerations indicated that not more than three of this list were likely to be chance coincidences.

The frequency distribution of α for the 101 selected Perseid meteors has been investigated and is summarized in Table I. It is evident that the observed distribution with respect to α extends over a wide range of values.

TABLE I

Distribution of Meteors with Respect to α

α	0°	10°	20°	30°	40°	50°	60°	70°
Number	1	7	6	4	10	12	17	
α	70°	80°	90°	100°	110°	120°		
Number	10	12	14	2	6			

Let us refer to Fig. 1(a) (plan). The value $h=45°$ was chosen as an average value for the Perseid radiant. The frequency of shower meteors to be expected in the interval α_1 to α_2 is proportional to the area between the corresponding curves. The actual number seen by the radar should be found by reducing this frequency by factors involving the range, the antenna pattern, and the angle α. The range factor is the subject of considerable discussion in the literature at present, and, while a reasonably fair estimate of the correction could be applied here, the scatter of the values in Table I does not seem to warrant it. A rough comparison between Fig. 1 and Table I does indicate a fair correspondence between numbers and areas and demonstrates that, on 32.7 Mc, the normal reflection law has little effect on the radar detectability of the brighter meteors.

The Geminid and Lyrid data have not been fully reduced as yet, but so far there has been nothing to con-

[12] The *apparent radiant* is defined by the direction of the observed meteor paths and is, hence, the observed radiant uncorrected for the effect of the earth's gravity; i.e. zenith attraction.

[13] F. L. Whipple, "Photographic meteor studies IV. The Geminid shower," *Proc. Amer. Phil. Soc.*, vol. 91, pp. 189–200; April, 1947.

tradict the conclusions we propose to draw from the Perseid data. On the other hand, the supporting evidence of the Geminid and Lyrid observations fills in some gaps in the Perseid material; partly because the slower velocities of the Geminids and Lyrids, 35 km per second and 48 km per second, respectively, compared to 61 km per second for the Perseids, provided us with different values of one of the parameters, and partly because the improved performance of the radar system brought out some detail on the radar display that was not available in the earlier run. Further significant information is available from dual-station observations made during the Lyrid shower, where two independent radar stations 57 km apart (Ottawa and Arnprior) were used in conjunction with visual and photographic observations.

The selected Perseid echoes were originally classified into six groups based on their general appearance.[4] These were lettered A to F, and it was found that there was a correlation between the form of the echo and the values of α. For example, echoes showing a range decreasing with time had α's less than 90°, and those with a range increasing with time had α's greater than 90°. These correlations were confirmed in the results obtained from the Geminid and Lyrid observations, and the original classification of echo types has more recently been somewhat altered and expanded to include a wider range of observational material.[5] While there is a great variety of echo forms, and many strong echoes exhibit an individuality of their own, it is possible to systematize most of the observed characteristics. The designations assigned in the revised classification are listed in Table II, and illustrated with examples in Fig. 7.

TABLE II

CLASSIFICATION OF METEOR RADAR ECHOES

Basic type—dependent on α
- "A"—indication of decreasing range or approach ($\alpha<90°$)
- "D"—indication of increasing range or recession ($\alpha>90°$)
- "U"—indication of both approach and recession ($\alpha\doteq 90°$)
- "E"—two or more discrete ranges, no motion evident ($\alpha\neq 90°$)
- "F"—one discrete range, no motion evident ($\alpha=0°$ to 180°)

Secondary characteristics—indicated by small letters and numbers following letter for basic type
- "h" = instantaneous head echo apparently moving with velocity of meteor
- "b" = moving echo with measurable and continuously variable duration
- "e"—two or more echoes at discrete ranges
- "f"—one echo at a discrete range
- "n"—nebulous or diffuse echo
- "s"—duration under 1 second
- 2, 3, 4, etc.—number of components.

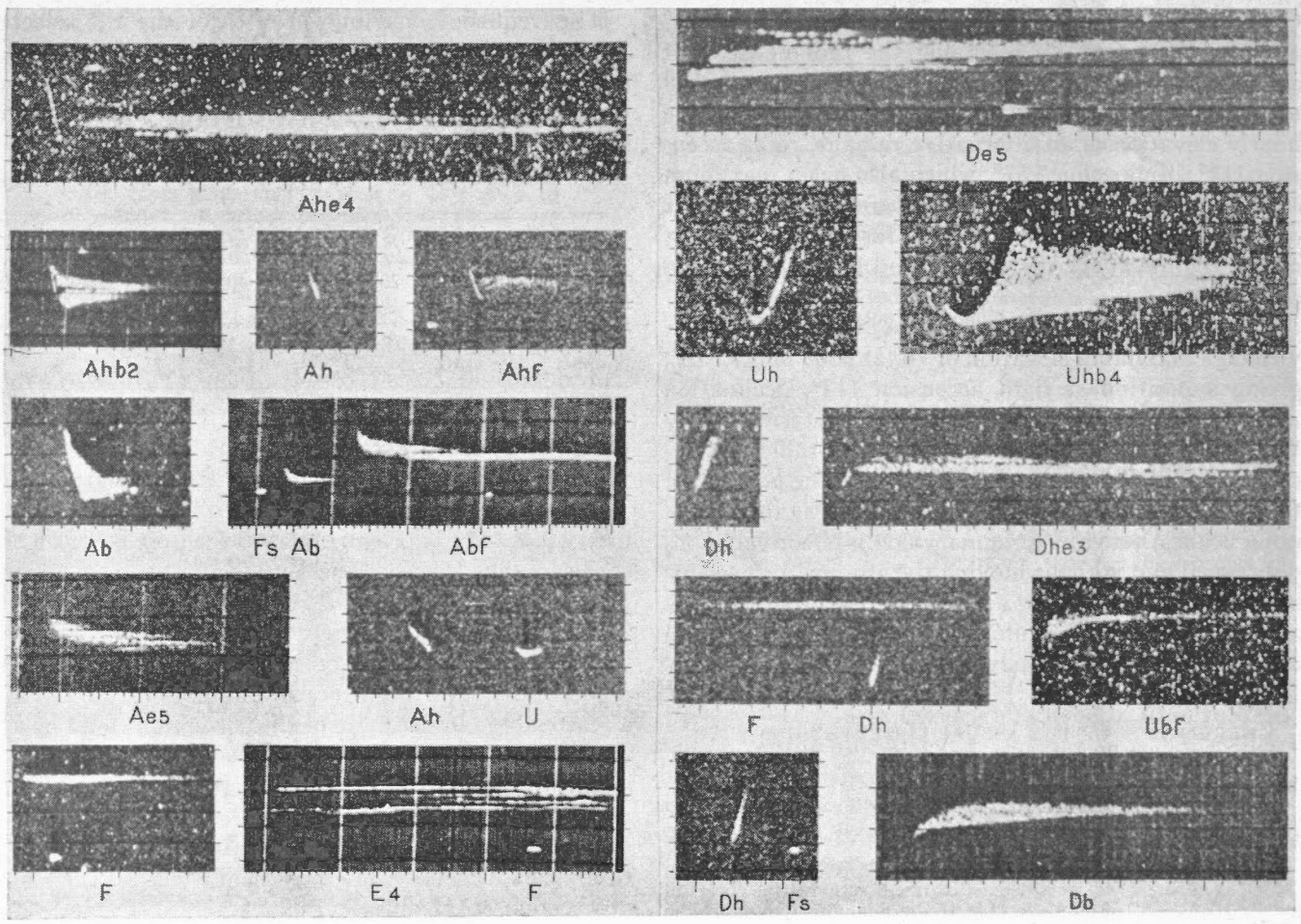

Fig. 7—Typical meteor echoes photographed on an intensity-modulated range-time display; range as ordinate, marked at 20-km intervals, time as abcissa, marked at one-second intervals.

The salient echo forms are described in more detail below.

(i) A large percentage of the bright and long-duration echoes shows evidence of a systematic change of range with time. As noted above, this property has been correlated with the observed α's. Echoes showing a decreasing range (i.e., approach) have been placed in type "A," while those with an increasing range, or recession, have been classified type "D." A less common form, exhibiting both approach and recession, has been called type "U".

(ii) Enduring echoes which do not fall into any of the above three types consist of one or more discrete components, each at an approximately constant but separate range. Those with two or more components at different ranges are called type "E," a numeral following the letter being used to indicate the total number of components observed. Enduring echoes at one range are type "F." The average range separation of the individual components of type "E" echoes is 3 to 4 km. Meteors producing echoes of type "E" average considerably brighter than those with type "F" echoes. Type "E" echoes, in general, correspond to meteors with α's differing considerably from 90°, but type "F" echoes may have α's of any value.

(iii) In considering compound echoes of type "A," "U," or "D," various classes of their component parts have been noted. A moving echo having no appreciable enduring characteristics, and with a range-time motion apparently corresponding to the geocentric velocity of the meteor is designated by "h." A moving echo whose duration varies continuously with range is designated by "b." The leading edge of the "b" characteristic may correspond to a velocity less than that of the meteor. Enduring components at approximately constant ranges are designated by "e" where two or more are observed, and by "f" where only one is present. In general, echoes with "b" characteristics have α's nearer to 90° than do those with "e" characteristics.

Apart from the general appearance and type of the echo, the two principal correlations with α involve the spread in slant range covered by the echo, and the mean delay in the appearance of the echo after the occurrence of the visible meteor. On the average, the spread in range exhibited by an echo is greater the more the corresponding α differs from 90°. For the Perseid echoes, where a spread in range could be measured, this corresponded to roughly 15 km of meteor path length for the *e* characteristic and 30 km of path length for the *b* characteristic, giving an over-all average radar path length of about 20 km. The average values of the time delay in the appearance of the echoes showed a definite increase as the corresponding values of α deviated from 90°, in spite of a considerable scatter of the individual delay values. Approximate mean delays of the appearance of the "e" and "f" characteristic for the Perseid meteors are listed in Table III.

TABLE III

α	Mean Delay
0°– 39°	10 seconds
40°– 59°	8
60°– 79°	6
80°– 99°	1
100°–119°	greater than 2

For the selected Perseid echoes, the mean duration varied directly with apparent meteor brightness. There appears to be a straight-line relation between the logarithm of the echo duration and the apparent visual magnitude of the meteor. Echoes of 35 seconds duration correspond to Perseids of apparent magnitude zero. Examination of the Geminid and Lyrid observations indicates that the mean echo duration also varies with the geocentric velocity of the meteor; the durations of the Lyrid and Geminid echoes being shorter, corresponding to their lower velocities. The majority of the long-duration echoes ("e" and "f" characteristics) exhibit a slow drift in slant range. These drifts are of the order of 1 km in 25 seconds and seem to be predominantly away from rather than toward the observer.

In general, the visual meteor path length is longer than the path length observed by radar (by a factor of the order of 2 for the Perseids) but there is considerable evidence to show that the great majority of radar echoes occur somewhere along the visual meteor path. Making this assumption, and by combining visual and radar data, possible limits in height were computed for the selected list of Perseid echoes. The frequency distribution of all heights between these limits is shown in Fig. 8. The dotted curve is drawn for the meteors with the

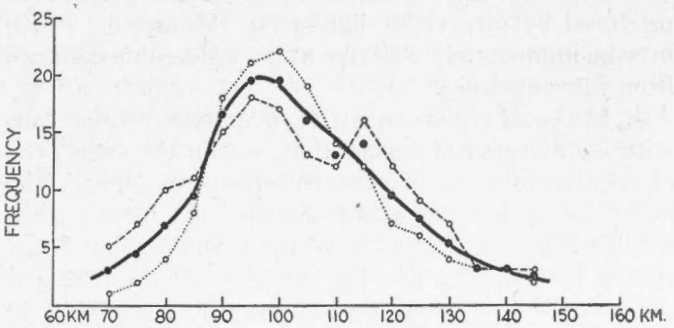

Fig. 8—Heights of enduring Perseid echoes. Solid curve—all selected echoes; dotted curve—echoes with more accurate visual observations; dashed curve—echoes with less accurate visual observations.

more accurate visual observations (about half the total number), while the dashed curve is drawn for the meteors less accurately plotted. The solid curve is the mean distribution for all the meteors. It will be noted that the maximum of the curve is considerably sharper for the better visual plots, indicating that a significant portion of the spread of this curve is due to observational error. By combining the known elevation of the radiant with the mean radar path length quoted earlier, we find that a bright meteor quite frequently produces enduring echoes extending over a height spread of 15 km. Let us assume a region, at least 15 km thick, in which endur-

ing meteor echoes are most likely to be produced. Each of the three curves in Fig. 8 places this region at heights between 90 and 105 km above sea level, with a maximum just under 100 km. Heights for fifteen Lyrid meteors indicate values of the same order but with the maximum somewhat lower. This agrees with earlier observations by Hey and Stewart.[8]

A Theory of Meteor Radar Echoes

We shall first outline a phenomenological theory of the mechanics of radar reflections from meteoric ionization, and then examine whether the assumptions made explain the observations satisfactorily. The following postulates will be used:

1. There is an M region (M for meteor), in the upper atmosphere, which is slightly below but overlapping the recognized E region, and in which the great majority of the radar echoes from meteors occur. The M region is considered to have physical properties which sustain the ionization caused by the passage of a meteor. These properties have a maximum effect over a height spread of 15 to 20 km, centered somewhere between 90 and 100 km above sea level. The region may have diurnal and annual fluctuations in height, thickness, and ionizing ability.

2. A meteoroid will produce a long, thin column of dense ionization in its passage through the M region. Two mechanisms for the production of this ionization are envisaged. The first is a kinetic energy transfer through collisions involving both meteoric and air particles, the action occurring in the immediate vicinity of the meteoroid. The second is a radiation energy transfer produced by ultraviolet light from the meteor, which may be immediately effective at a considerable distance from the meteoroid.

3. In the M region are striae, or patches, which constitute a fine structure such that, within the striae, the physical properties of the atmosphere emphasize the formation and maintenance of meteoric ionization. No specific shape, thickness, extent, or orientation is assigned to these striae. They may exist as localized patches only, or they may extend throughout the M region in the form of horizontal, vertical, or inclined layers or rays. Their effective thickness is of the order of 1 km or less and the spacing between striae is of the order of 5 km.

4. The rate of expansion of any ionization cloud produced by the meteor is greatest at the top of the M region and decreases toward the bottom.

Fig. 9 is intended to show, diagrammatically, the successive stages in the growth of the ionized column, at times $t=1$, 3, and 10 seconds, say.

Immediately after the passage of the meteor, which normally takes less than 1 second to pass through the whole M region, the cloud of ionization is in the form of a long, thin column. This column reflects the radar wave most efficiently when viewed at an angle $\alpha=90°$. The received signal power is proportional to R^{-4}, which can be deduced from purely geometrical considerations.[14] The effective reradiation pattern (drawn in the plane containing the meteor path and the observer) of the column at $t=1$ second is such that the echoes from most of the meteors will not be detected at all for α's varying more than a few degrees from 90°.

Now, suppose we consider a meteor with $\alpha=70°$ at the midpoint, and which has produced a radar echo for 10 km on either side of the midpoint. This echo will appear to have a typical leading edge curl ("b" characteristic), which generally represents an effective velocity somewhat less than the actual meteor velocity. On the basis of our assumptions, this retarded appearance is due to the slower growth of the ion cloud in the lower part of the M region. When viewed at a slight angle away from $\alpha=90°$ the radiation pattern is initially quite narrow, but quickly broadens out, and the broadening occurs first for the higher parts of the path. Thus there will be a slight but nevertheless real lag in the appearance of this echo, even for meteors with α near the 90° value. These lags might be measured in hundredths of seconds for the higher parts of the echo and tenths for the lower parts, and increase as α diverges from 90°.

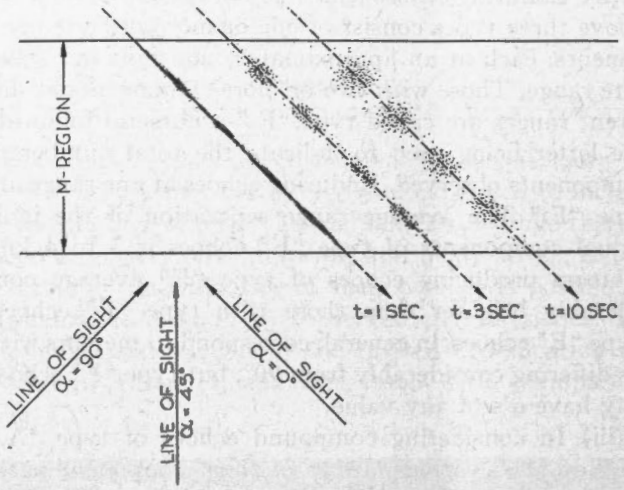

Fig. 9—Change of meteoric ionization clouds with time.

In Fig. 9 the same meteor path is represented at time $t=3$ seconds. The ionization continues to expand as described in postulate 4, but the densities are rapidly thinning out. At time $t=10$ seconds, the densities between the striae may be so thin that a radar wave will not be reflected with detectable amplitude, despite the broadening pattern, but the striae patches may still be dense enough. Viewed from $\alpha=90°$, these patches may not be resolvable, since they may overlap in slant range. However, viewed from a low α direction, these striae patches may eventually build up to detectable and discrete target areas, provided their densities remain adequate.

[14] J. P. M. Prentice, A. C. B. Lovell, and C. F. Banwell, "Radio echo observations of meteors," Monthly Notices of the Royal Astronomical Society, vol. 107, no. 2, pp. 155–163; 1947.

The delays in appearance of the echoes will be successively greater for the lower patches and may be measured in seconds. The criterion for detectability is a combination of patch ionization density and solid angle of the patch as viewed from the radar. The received signal power in this case would probably be proportional to R^{-4}, as in the usual radar equation,[15] rather than R^{-3} for a thin cylinder.

Thus, only the brighter meteors viewed from low α's can cause echoes with "e" characteristics because several seconds are needed to blow up the patches to detectable targets, densities are rapidly thinning out in the process, and the effective range attenuation factor is increasing from R^{-3} to R^{-4}. The "Ae" echoes are considered to be the well-behaved ones and the processes described in the above paragraph account for them satisfactorily. The "E" echoes are thought to be cases in which the ionization is unevenly distributed through the various striae. The "F" echoes will occur when only one patch becomes detectable, or when the more complex characteristics of an echo near $\alpha = 90°$ are lost because of lack of range resolution.

Most of the visual meteors produce visible light that rises and falls in a continuous manner from start to finish of the trail. None of the meteors considered here exhibited luminosity bursts, which might explain the appearance of the "e" characteristic.

By assuming an arbitrary rate of diffusion of the ionized clouds in all directions, and then evaluating the solid angles of the clouds as viewed from different α's and at increasing time intervals after the passage of the meteor, it is possible to show that a time will come when, if a patch is sufficiently dense to be detectable at all, it will be detectable from any α. Examination of Fig. 9 will confirm qualitatively that the patches eventually should become roughly spherical. The dual-station results have confirmed this point; practically every echo that endured for more than five seconds at the Arnprior station was also displayed on the Ottawa radar film; the echo times and characteristics corresponded, though the ranges and "e" component separations varied as would be expected.

In any discussion of the origin and maintenance of the striae in the M region, the possible effect of the upper-atmosphere winds must not be forgotten.[8] The existence of such winds is evident from the motions of enduring meteor trains observed visually, the most recent compilation of observational data having been made by Olivier.[16] Motion in practically any direction, often turbulent in nature, and with velocities of the order of 200 km per hour (55 meters per second), is common. The original thin column of meteoric ionization is undoubtedly deformed by these winds, but that this deformation is entirely responsible for a number of discrete echoes appearing at such short range intervals, sometimes within a few tenths of a second, and maintaining identity over appreciable periods of time (even when viewed from two stations as in the Lyrid observations) seems hardly likely. It should also be pointed out that the frequent appearance of the F-type echo for meteors with low α's and visual path lengths in the neighborhood of 45 km indicates strongly the existence of sharper discontinuities in the physical conditions favorable to enduring echo production than would seem possible on the basis of wind motion alone.

In the case of the "h" characteristic (first noted by Hey and Stewart[8] for the Giacobinids) there is usually no measurable endurance of the echo, and for a very bright meteor this echo may appear well outside the M region. Since the motion of the "h" echo corresponds to the geocentric velocity of the meteor, it must be closely associated with the moving meteoroid. It is probable that the diffusion of ionization produced by collision is too slow to produce immediately a cloud big enough to reflect the 9-meter radio waves. We believe that instantaneous ionization by intense ultra-violet light at some distance from the meteor head may well explain the "h" characteristic echo.

It will be of interest now to examine, in more detail, the predicted appearance of the various echo forms. We shall assume that the echoes appear on a range-time display with a scale ratio of 10 km = 1 second (form factor = 10). Assuming a constant velocity for the meteor over most of its visible path, an assumption justified by photographic determinations of meteor velocity, the motion of the meteor on the range-time diagram will trace out a hyperbola. The form of this curve will vary with the geocentric meteor velocity v, and the perpendicular distance of the observer from the meteor path R_0 at time t_0. This hyperbola, $R^2 = R_0^2 + v^2(t - t_0)^2$, is the framework upon which any meteor echo is built.

A series of theoretical echoes has been plotted in Fig. 10, using typical values of the significant parameters and applying delays in the appearance and disappearance of the echo similar to those observed. The plotted echo outline has also been modified to take account of instrumental effects such as defocus and overshoot[17] of a bright trace, and the consequent masking of detail which would otherwise appear.

General Discussion

Assuming all the radar echoes to be due to meteors and to obey the normal reflection law, a satisfactory position of the Geminid radiant has been determined.

[15] K. A. Norton and A. C. Omberg, "The maximum range of a radar set," Proc., I. R.E., vol. 35, pp. 4–24; January, 1947.

[16] C. P. Olivier, "Long enduring meteor trains," *Proc. Amer. Phil. Soc.*, vol. 85, pp. 93–135; January, 1942; and vol. 91, pp. 315–327; October, 1947.

[17] Video overshoot was introduced in an attempt to obtain a three-dimensional graph of the echo. The length of the black shadow above the echo is a measure of the echo signal strength in excess of the clipping level.

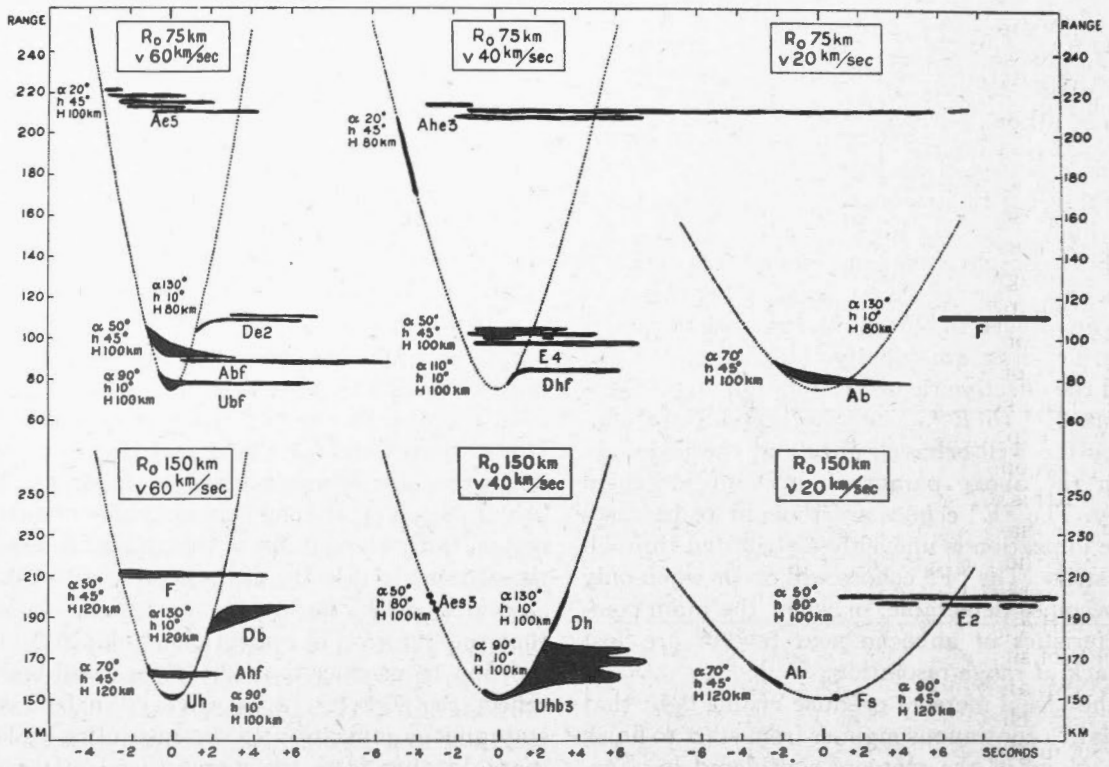

Fig. 10—Typical meteor echo forms. Representative echo types drawn by assuming various values of the following parameters, as indicated on the diagram:
R_0 = perpendicular distance from observer to meteor path
v = geocentric velocity of meteor.
α = angle between visual meteor path and line of sight.
h = angular elevation of the meteor radiant.
H = height of visual meteor path above sea level.
Basic hyperbolas have been shown as dotted curves. A distance on these hyperbolas corresponding to the assumed visual path length of 45 km can be drawn at any point by marking off time intervals of 0.75 second for v = 60 km per second, 1.12 seconds for v = 40 km per second, and 2.25 seconds for v = 20 km per second.

Doubt has been expressed in the past that all the transient echoes seen on frequencies below 50 Mc are due to meteors. The possibility of this cannot be denied, but by treating all the echoes as meteor echoes we have reached the conclusion that they all behave statistically as the known meteor echoes do. The myriads of small echoes may be due to telescopic meteors, or to nonluminous particles passing through one or more of the ionized regions.

As will be apparent from the hourly-rate curves of Fig. 4, the maximum ratio of shower echoes to sporadic echoes during the Geminid shower was of the order of 1 to 1. On the other hand, the ratio of visual shower meteors to sporadic meteors during the same night was between 2 to 1 and 3 to 1. The radar set can see echoes from meteors well below the visual limits, provided that the meteor paths are favorably oriented. The radar ratio should at least be equal to, if not greater than, the visual ratio during the periods when the radiant was at a favorable elevation, if one assumed that the size distributions of the shower particles and the sporadic particles were similar. Another observed fact is that the percentage of radar echoes of duration 1 second and longer during the shower periods was much higher than during typical nonshower periods (15 to 20 per cent, as compared to 8 to 10 per cent), indicating the presence of a greater percentage of large particles in the shower. One concludes, therefore, that there actually is a smaller percentage of faint meteors in the shower stream than in the sporadic background. This conclusion lends weight to the suggestion[18] that the established annual meteor streams, which have meteoric particles well distributed around their orbits and which originated thousands or even millions of years ago, contain few small particles. A younger shower, such as the Giacobinids which appeared in great strength in October, 1946, should accordingly yield a radar echo ratio more in line with the visual ratio.

Deep fluctuations in the signal strengths of the long-enduring echoes are frequently observed. These fluctuations are usually random in period and amplitude and are presumed to be due to the destructive interference effects of the signal received from various parts of the ionized cloud as it grows. Distortion by upper-atmosphere winds could contribute to this effect. Occasionally, a fairly regular amplitude flutter, of the order

[18] F. G. Watson "Between the Planets," Blakiston Co., Philadelphia, Pa., 1941; pp. 134–137.

of 5 to 10 cps, is superposed on the random fluctuations. As this is observed seconds after the meteor has occurred, it cannot be due to doppler effects from the moving meteor itself, athough it might be due to the doppler effect produced by the expansion of the ionized column. Successive rf pulses emitted by the radar transmitter are not coherent, so, if there is a true doppler effect, the reference phase must come from the ionized cloud itself. If one were to imagine that the central part of the cloud remains somewhat denser than the rest, and that the signal returned from this central part provides the reference phase, then, on the assumption that the interfering signal comes from near the expanding edge, one deduces that the rate of expansion is at least of the order of 50 to 100 meters per second. This analysis is, admittedly, highly speculative at this stage. Interference effects from the *moving* meteor have been detected by Ellyett and Davies,[19] using the already-formed part of the meteor ionization to supply the reference phase for the signal received from the latter portions as the meteor moves across the line of sight.

A possible explanation of the observed fact that most of the enduring echoes increase slightly in range before they fade out might be that the ionization density decreases below the critical density for the radio frequency employed, thus producing an apparent increase in range similar to the increase in virtual height of ionospheric records as the frequency is increased. We think that the critical-density hypothesis explains why workers using higher frequencies observe very few enduring echoes. The critical density of the cloud increases as the square of the frequency, so that a cloud detectable on 32.7 Mc will certainly remain visible much longer than on 72 Mc. As a consequence, we would expect fewer and fewer "e" characteristic echoes as the radio frequency is increased. Another way of stating this is that fewer echoes with α's diverging widely from 90° will be seen. On the other hand, as the frequency is lowered below 32.7 Mc, we would expect the "e" characteristic echoes to increase in number and duration. In particular, a very bright meteor should be capable of producing a large cloud of ions which might linger for hours with densities sufficient to reflect radio waves in the 2- to 25-Mc band. Such a cloud would drift with the winds, and, as it approached and receded from a vertical-incidence ionospheric station, the characteristic "abnormal-*E*" echoes would be obtained. We agree with Pierce[20] and with Appleton and Naismith[21] that meteoric ionization alone could thus be responsible for many of the "abnormal-*E*" effects observed in the 2- to 25-Mc band.

[19] C. D. Ellyett and J. G. Davies, "Velocity of meteors measured by diffraction of radio waves from trails during formation," *Nature*, vol. 161, pp. 596–597; April 17, 1948.

[20] J. A. Pierce, "Abnormal ionization in the *E*-region of the ionosphere," Proc. I.R.E., vol. 26, p. 892; July, 1938.

[21] Sir Edward Appleton and R. Naismith, "The radio detection of meteor trails and allied phenomena," *Proc. Phys. Soc.*, vol. 49, pp. 461–473; May, 1947.

Doppler Whistles

A remark on the doppler whistles from meteors, observed by many workers, seems in order here. A simple geometrical analysis shows that a whistle decreasing in pitch corresponds to an approaching meteor, and a whistle increasing in pitch to a receding meteor.[21] In some instances, it is probable that the whistle does represent the velocity associated with the moving meteor, but we feel that often the velocity deduced from the whistles will represent an apparent velocity[22] which is actually a measure of the leading-edge envelope ("b" characteristic) of the growth of the ionized clouds. Thus the whistle velocities would, in general, be somewhat less than the actual meteor velocities, and might even indicate fictitious decelerations. It should be emphasized, however, that these remarks are intended to apply to moving radar echoes and doppler whistles which extend over an appreciable time interval of the order of seconds, or which are comparatively remote from the t_0 point. The range resolution of the radar echoes obtained over a short time interval about the t_0 point is insufficient to predict the reliability of the corresponding doppler whistles. The doppler whistles might well yield accurate readings of velocities in the immediate vicinity of this point because, as has been shown above, the delay in echo appearance is least where $\alpha = 90°$, i.e., at t_0.

Some of the stronger meteors produced signals on the range-time display independently of the transmitter pulse, as was indicated by the appearance of noise on the film from zero to maximum range during the radar echo time. In some cases, the noise was strong enough to depress the inherent receiver noise by virtue of the video overshoot effect. Whether this noise actually emanated from the ionized cloud itself or was a reflection of some distant transmitter signal is not clear at present. The noise does appear to start 1 second or so *after* the passage of the meteor and to last as long as the enduring radar echo. The length of the noise pulses appears to be 2 or 3 microseconds, which is the limit of resolution of the receiver (bandwidth 300 kc). Similar bands of noise have appeared at times when no corresponding radar echo was seen, and these bands might have been due to meteors beyond the limits of the range display.

Conclusion

This paper is admittedly a preliminary analysis of the general problem, made chiefly from the observational viewpoint. An indication has been given of the value of the study of echo forms and their statistics in the detailed investigations of daytime meteors. The observational techniques employed are capable of yielding further information concerning the microscopic

[22] J. A. Pierce, "Ionization by meteoric bombardment," *Phys. Rev.* vol. 71, pp. 88–92; January 15, 1947.

factors involved (e.g., electron and ion densities) which have been discussed only superficially here, but this material will be left for a future paper.

Acknowledgment

It should be pointed out that there is a lengthy list of those who assisted in the construction and operation of the equipment, in the visual observations, and in the reduction of the data, and who through their enthusiasm contributed materially to the success of the over-all program. We should like, in particular, to acknowledge the assistance of Miss M. S. Burland, who directed the visual observers, and of E. L. R. Webb, who was in charge of the construction of the radar equipment.